

國立臺灣大學電機資訊學院資訊工程學系

碩士論文

Department of Computer Science and Information Engineering

College of Electrical Engineering and Computer Science

National Taiwan University

Master Thesis

使用雙向卷積長短期記憶網路的全持續時間閃焰檢測、  
分類和區域提取

Full Duration Flare Detection, Classification and Region  
Extraction using Bidirectional Convolutional LSTMs

黎軒喬

Nikita Mikhaylovich Galayda

指導教授：莊永裕 博士

Advisor: Yung-Yu Chuang Ph.D.

中華民國 111 年 9 月

September, 2022

國立臺灣大學碩士學位論文  
口試委員會審定書

使用雙向卷積長短期記憶網路的全持續時間閃焰檢測、  
分類和區域提取

Full Duration Flare Detection, Classification and Region  
Extraction using Bidirectional Convolutional LSTMs

本論文係黎軒喬君（學號 R09922164）在國立臺灣大學資訊工程  
學系完成之碩士學位論文，於民國 111 年 9 月 23 日承下列考試委  
員審查通過及口試及格，特此證明

口試委員：

莊永裕

（指導教授）

葉正聖

吳賦哲

系主任

洪士瀨



## Acknowledgements

I would like to express my gratitude to my advisor, Dr. Chuang, whose advice and guidance were instrumental to completing this research. They provided me the freedom to pursue the topic of my interest, while still keeping my thesis in check with constructive criticism and supervision. With his help and trust, this paper came into fruition.

I'd also like to thank Dr. Yeh and Dr. Wu, for being part of the committee for my thesis defense. Their time and knowledge in the field are appreciated and helped me in improving the research.

Lastly, I'd like to thank the members of the CMLab who provided the necessary tools for the experiments for this thesis.





# Abstract

Solar flares have been one of the focal interests among researchers, as they have a profound effect on Earth. Both prediction and detection of solar flares are well studied topics in the field, however detecting the full duration of a flare has yet to be explored. In this research, we propose an automatic system for detection, classification, and extraction of solar flare regions for their entire duration using bidirectional LSTMs on images in the Extreme Ultra Violet range. Unlike numerous current research, we use images within a short time window to train our network. Moreover, a custom dataset generation method has also been proposed, which is able to create sequences of images of the full sun during a flare, as well as flaring regions specifically. In order to exploit both the temporal and spatial information of the flare event, we use multiple convolutional LSTMs, resulting in a relatively lightweight model. Our model can successfully detect flares for their approximate duration using only image data, which is a novel approach at an unexplored problem in the field.

**Keywords:** ConvLSTM, Solar Flare, Full Duration, Multi Class Classification



# Contents

	<b>Page</b>
<b>Acknowledgements</b>	<b>3</b>
<b>Abstract</b>	<b>5</b>
<b>Contents</b>	<b>6</b>
<b>List of Figures</b>	<b>9</b>
<b>List of Tables</b>	<b>11</b>
<b>Denotation</b>	<b>13</b>
<b>Chapter 1 Introduction</b>	<b>1</b>
<b>Chapter 2 Related Work</b>	<b>3</b>
2.1 Solar Event Detection . . . . .	3
2.2 Solar Flare Detection . . . . .	4
2.3 Solar Flare Prediction . . . . .	4
2.4 Solar Flare Duration Detection . . . . .	5
<b>Chapter 3 Data Acquisition</b>	<b>7</b>
3.1 Solar Dynamics Observatory . . . . .	7
3.2 SDO Images Dataset . . . . .	7
3.3 Dataset Creation . . . . .	8
3.3.1 Flare Data Retrieval . . . . .	8

3.3.2	Flare Image Sequence Creation . . . . .	9
3.3.3	Data Augmentation . . . . .	10
3.3.4	Datasets . . . . .	11
<b>Chapter 4</b>	<b>Methods</b>	<b>13</b>
4.1	Goal . . . . .	13
4.2	Convolutional LSTM . . . . .	13
4.3	Bidirectional Convolutional LSTM . . . . .	14
4.4	Model Architecture . . . . .	14
4.5	Region Extraction . . . . .	15
<b>Chapter 5</b>	<b>Experiments and Results</b>	<b>17</b>
5.1	Validation Data . . . . .	17
5.2	Evaluation Metrics . . . . .	17
5.2.1	Flare Classification . . . . .	17
5.2.2	Flare start and end prediction . . . . .	18
5.3	Results . . . . .	19
<b>Chapter 6</b>	<b>Conclusion</b>	<b>25</b>
	<b>References</b>	<b>27</b>
	<b>Appendix A — Additional Data</b>	<b>31</b>
A.1	Flare data retrieved from HEK . . . . .	31
A.2	Raw Confusion Matrices . . . . .	33
A.3	A demonstration video . . . . .	35
	<b>Appendix B — Formulas</b>	<b>37</b>
B.1	Evaluation Metric Formulas . . . . .	37









# List of Figures

3.1	Flare data query pipeline . . . . .	9
3.2	Flare image sequence creation pipeline . . . . .	10
3.3	Single frame data augmentation visual . . . . .	11
4.1	A ConvLSTM Cell . . . . .	14
4.2	Our model architecture . . . . .	15
5.1	Confusion Matrices for the tested models of flare start detection. The representations are scaled into a $[0, 1]$ range. The confusion matrices with raw values can be found in Appendix A. . . . .	20
5.2	Confusion Matrices for the tested models of flare start detection cutouts. The representations are scaled into a $[0, 1]$ range. The confusion matrices with raw values can be found in Appendix A. . . . .	23





## List of Tables

3.1	Original number of flare events . . . . .	9
3.2	Number of flare event image sequences after data augmentation . . . . .	11
3.3	Flares included in our datasets . . . . .	12
5.1	Evaluations of the NMX6 model . . . . .	21
5.2	Evaluations of the HMX6 model . . . . .	21
5.3	Evaluations of the NCMX6 model . . . . .	21
5.4	Evaluations of the NCMX12 model . . . . .	21
5.5	Average errors for flare start and end predictions of all detected flares . . . . .	24
A.1	Flare data retrieved from HEK . . . . .	32





# Denotation

Å	Angstrom
SDO	Solar Dynamics Observatory
HEK	Heliophysics Events Knowledgebase
HMI	Helioseismic and Magnetic Imager
AIA	Atmospheric Imaging Assembly
<i>MLDSO</i>	A Machine Learning Dataset Prepared From the NASA Solar Dynamics Observatory Mission
CNN	Convolutional Neural Network
LSTM	Long Short-Term Memory
ConvLSTM	Convolutional Long Short-Term Memory
Bi-ConvLSTM	Bidirectional Convolutional Long-Short Term Memory





# Chapter 1 Introduction

Solar flares have been extensively researched by the scientific community not only to study their nature, but also to analyse their potential impact on Earth. Prediction of solar flares within a specific time window is a continually explored problem that has had improved results over the last decade, especially with the introduction of novel machine learning methods. The massive amounts of solar data that has been gathered up to today provides vast opportunities when used in junction with the data demanding machine learning algorithms, and the work on solar flares is one of such opportunities.

Although there has been substantial focus on the study of solar flares, the researches are limited in their nature. Most studies deal with detecting solar flares at Active Regions of the sun, and work within a lengthy time period, usually 24 hours. Moreover, despite the fact that solar flare prediction is a well studied topic, there has been little to no research in regards of determining the full duration of flares. In this research, we tackle the issue of detecting, classifying and determining the full duration of flares.

Solar flares are sudden outbursts of magnetic energy from the solar corona which may be classified into the categories A, B, C, M, and X, in ascending magnitude where class X solar flares are the most powerful. While flares of classes A, B, and C are relatively harmless to the Earth, the other two classes may have the potential to disturb the the Earth's

ionosphere, which can cause disruptions in the radio communications [1]. Therefore, it is imperative that methods for predicting solar flares are developed. In the recent years, there have been multiple researches aiming to predict whether or not a solar flare will occur in some time window. It has been demonstrated that CNN models which process image data of the sun can be useful in that task [2]. Besides using computer vision models, LSTM models, which use magnetic parameters without any image data, were also able to produce favorable results [14].

Due to the lack of research in this niche, there are no readily available datasets. Therefore, we created our own pipeline and dataset design fit for our task. We use the Machine Learning Dataset Prepared From the NASA Solar Dynamics Observatory Mission [8] as the source of the imaging data, and the Python package SunPy [24] for the queries of the flaring events. By combining the two, we were able to create a dataset comprising of image sequences prior to and during the flares from years 2010 to 2018. Since solar flares greatly change throughout their flaring period, there is a plethora of not only visual, but also temporal information to be exploited. Hence, our approach uses Bidirectional Convolutional LSTMs, which make use of both the spatial and temporal information when analysing image sequences.





## Chapter 2 Related Work

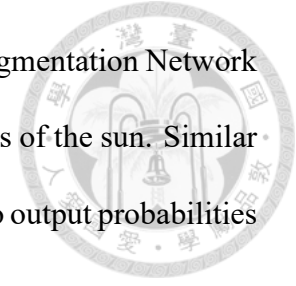
### 2.1 Solar Event Detection

A wide range of methodologies have been proposed for using machine learning models for solar event detection. Models such as Faster R-CNN, which produce great results on the PASCAL VOC 2007 dataset [19], has been used to detect solar events [12]. Armstrong *et al.* [4] created a model similar to the VGG19 in order to classify solar images in the  $H\alpha$  belonging to the classes Quiet, Prominence, Filament, Sunspot, or Flare ribbon. They achieved excellent results, and demonstrated that CNNs are highly useful in the classification of solar image data.

Baek *et al.* [5] used a custom labeled dataset to detect coronal holes, sunspots and prominences on the surface of the sun. The authors utilized Faster RCNN and SSD models in junction with the ResNet 101 for feature extraction to perform the detection task. Since solar data is far too different from the Imagenet dataset that these models were trained on originally, the authors trained them from scratch, unable to benefit from transfer learning. The study reached favorable results for the detection of the three classes, showing the potential of using CNNs in solar event detection.

The task of solar event detection has also been approached by segmentation. Mackov-

jak *et al.* [15] developed a U-Net inspired Solar Corona Structures Segmentation Network (SCSS-Net) [15] which segments the coronal holes and active regions of the sun. Similar to a U-Net, the authors used Convolution and Deconvolution blocks to output probabilities of each pixel belonging to a specific class [15].



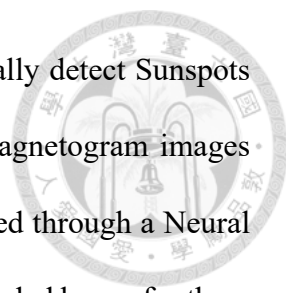
## 2.2 Solar Flare Detection

Early studies tackling solar flare detection used multi-layer perceptrons, radial basis functions, and support vector machines with carefully constructed features and human selected datasets [17]. Although they reach high accuracy rates, they were limited in their applicability due to the amount of hand crafted features necessary for the model. For the past decade, the focus has shifted from solar flare detection, to flare prediction, which is a useful tool used in order to prepare for the potential impacts of the flares.

## 2.3 Solar Flare Prediction

When it comes to solar flare prediction, a range of machine learning models have been applied. Jonas *et al.* [10] proposed using combinations of different types features to predict solar flares. The authors combined physical features of the active regions, such as total unsigned current helicity, flare history of the region, as well as HMI and AIA images. The study experimented predicting solar flares within a 2 and 24 hour windows using different combinations of the aforementioned features. A linear classifier was used, which yielded True Skill Scores (TSS) of above 0.8, similar to previous studies.

Abed *et al.* [2] proposed an automatic approach to predicting whether or not a solar



flare will occur within 24 hours. The created a system to automatically detect Sunspots and Active Regions of the sun by using HMI Intensitygram and Magnetogram images respectively. After the detection, the two groups are combined and fed through a Neural Network, where Sunspots in the Active Regions are detected and bounded boxes for them created. These groups of Sunspots are then processed by a CNN to determine whether or not they will produce a flare of class C or higher. This approach produced great results, with the maximum accuracy being 90

## 2.4 Solar Flare Duration Detection

Research on the durations of solar flares is scarce. Reep *et al.* [18] studied prediction of the remaining duration of an ongoing flare. The authors use the light curves and their flux values up to a certain point, and predict how long the flare will last. The study defines 5 time points of a flare's lifetime namely,  $t_0$ ,  $t_1$ ,  $t_2$ ,  $t_3$ , and  $t_4$ , where  $t_0$  is the start of the flare,  $t_1$  is when the light curve derivative is at its maximum,  $t_2$  is the peak of the flare,  $t_3$  is when the light curve derivative is at its minimum, and  $t_4$  is when the derivative returns to zero. The authors then train a random forest regression model to predict  $t_4$  (end of the flare) from either  $t_2$  (peak of the flare) or  $t_3$  (downward slope), producing predictions within 2 minutes of the true end of the solar flare.

As far as we know, there has been no research concerning the use of CNN or LSTM models in regards to determining the duration of solar flares.





## Chapter 3 Data Acquisition

### 3.1 Solar Dynamics Observatory

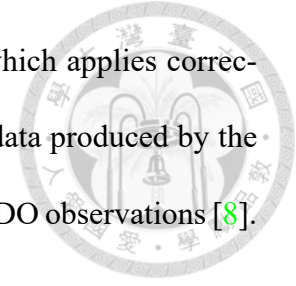
Many of the studies concerning solar flare prediction and/or detection, including ours, make use of the image data from the NASA's Solar Dynamics Observatory (SDO). The SDO collects data about the magnetic fields of the sun in multiple by orbiting a spacecraft around the star. SDO consists of three main research instruments, the Atmospheric Imaging Assembly (AIA), Extreme Ultraviolet Variability Experiment (EVE), and Helioseismic and Magnetic Imager (HMI)), which, besides other data, all produce image data of the sun in different wavelength bands, allowing it to capture a range of phenomena [16]. Our study uses images in the wavelengths of

Since our study focuses on flares, we chose to use the images from the 94Å channel of the AIA, which primarily observe the ions of the flaring corona [13]. Moreover, we use the images from the HMI instrument which focuses on Sunspots and Active Regions [20].

### 3.2 SDO Images Dataset

Since the data produced by the SDO is not properly processed for direct use in machine learning, we use the "Machine Learning Dataset Prepared From the NASA Solar

Dynamics Observatory Mission” dataset created by Galvez *et al.* which applies corrections, downsamples, and temporally and spatially synchronizes the data produced by the SDO, resulting in a dataset of image data for each wavelength of the SDO observations [8].



## 3.3 Dataset Creation

### 3.3.1 Flare Data Retrieval

Since there is no readily available dataset for determining the full duration of solar flares, one was created for the purpose of this study. As shown in Figure 3.1, in order to find the information on the flares, we utilized a Python SunPy [24] package to query the HEK (Heliophysics Event Knowledgebase) [9] for flares starting from year 2010 and ending in 2018, in order to only include the flares for which images can be found in the *MLDSDO*. The query returns numerous data points, a subset of which was kept. Notably, event start time, event end time, flare class, and flare coordinates were retained. A full list of the flare data points that were preserved, and their explanations, can be found in the Appendix A. After the query, the results with errors and duplicates were filtered out, leaving 6257 C class, 638 M class, and 38 X class flares. Additionally, two new flare classes were created. The N flare class was created to represent a Quiet event (no flare) and the H flare class represents the hybrid class including N and C class flares. To create the list of N flares, the list of C-class flares was used to shift the flare start and end times 12 hours earlier. To create the H flare list, the C and N flare lists were combined. The flare data was saved in a CSV format to a local database, with one CSV file per flare class. The number of each class flare event can be seen in table 3.1.

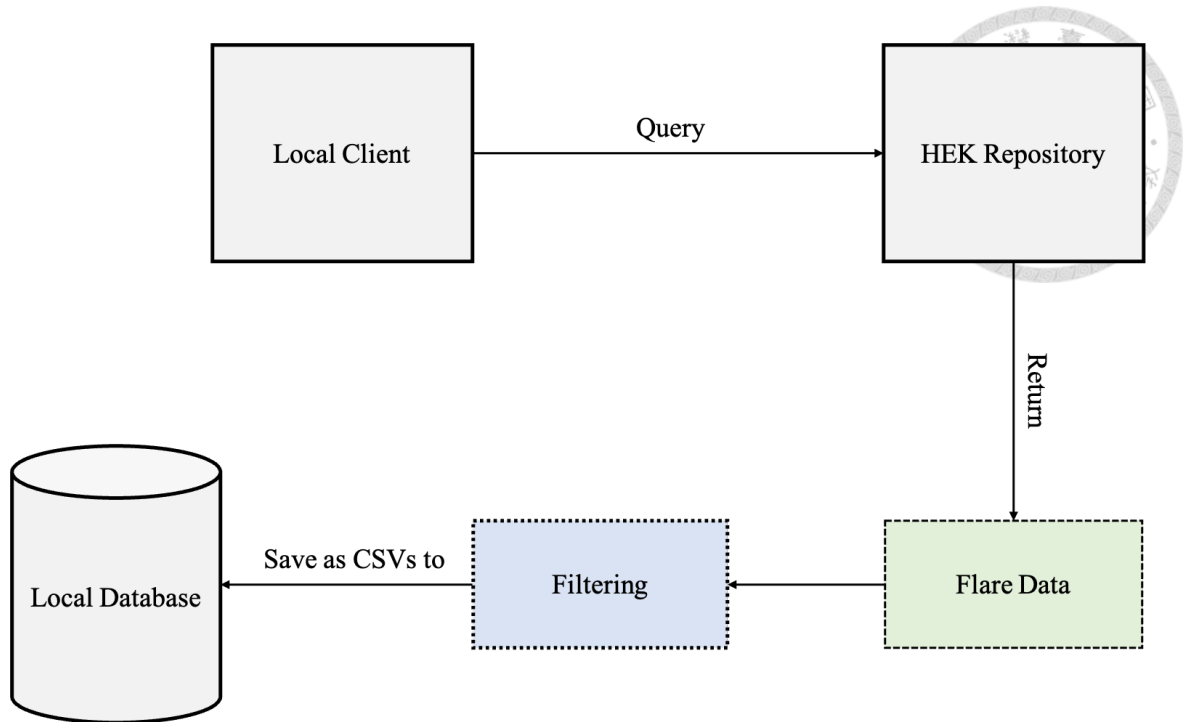


Figure 3.1: Flare data query pipeline

Table 3.1: Original number of flare events

Flare class	Number of events
C	6257
M	638
X	38
N	6257
H	12513

### 3.3.2 Flare Image Sequence Creation

With the flare lists, flare information, and the solar images from *MLDSDO* ready, image sequences of flare events could be commenced. In order to allow for flexibility, we created a pipeline which can create a sequence of  $N$  images in  $94\text{\AA}/1600\text{\AA}/\text{HMI}$  wavelengths starting from time  $T$  and moving backwards or forward in time. Images in the *MLDSDO* are provided at a 6 minute cadence, and therefore it is not likely that there will be images exactly at time  $T$ , meaning alignment needed to take place. Moreover, there were gaps in data where some images were missing. To overcome these obstacles, we found closest images to the time  $T$  and moved  $N$  timesteps forward or backward in time.

If an image for a given time was missing, it was skipped. After  $N$  timesteps, if the number of collected images was not equal to  $N$ , the remaining gaps were filled with the collected images. As a result, a sequence of  $N$  images is created. A visual representation of the image sequence creation process is represented in figure 3.2.

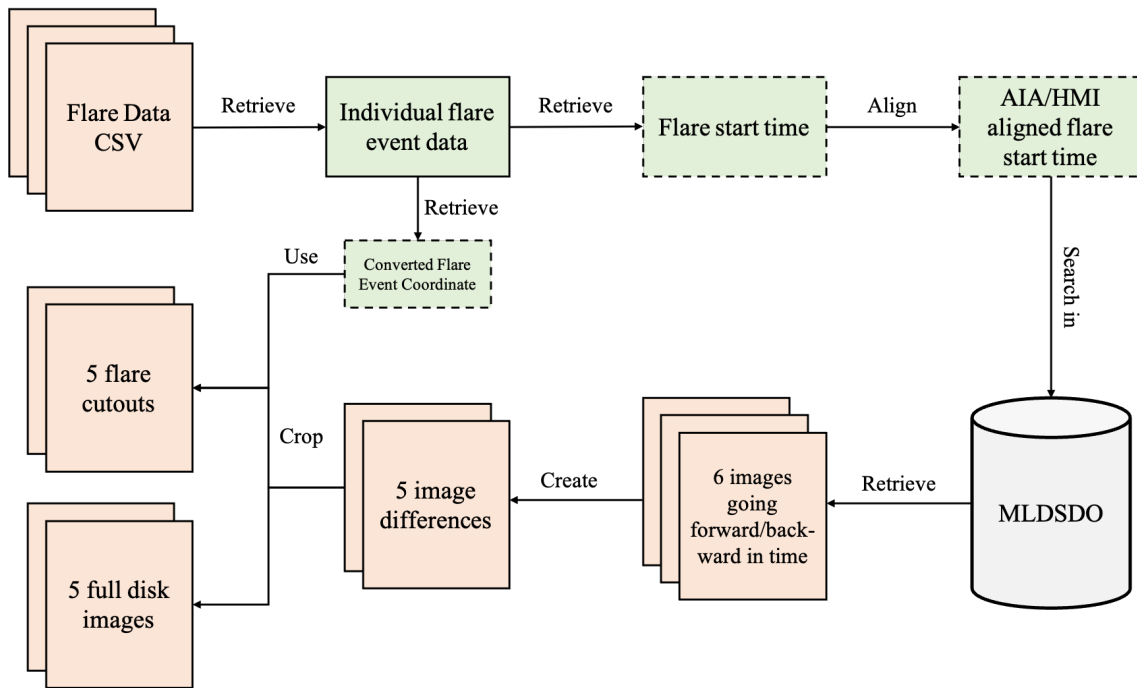


Figure 3.2: Flare image sequence creation pipeline

### 3.3.3 Data Augmentation

Higher magnitude flares occur much rarer than weak ones, leaving us with a highly imbalanced dataset. In order to combat the disproportionality of the training dataset, we used a data augmentation inspired by Aniyani *et al.* [3]. Our goal was to have at least 10,000 of both full disk image, and flare cutout image sequences for each flare class. To achieve that, for each flare event, we rotated image sequences by relative steps ( $\approx 180^\circ$  for C class flares,  $\approx 12^\circ$  for M class flares and  $\approx 1^\circ$  for X class flares) until a full  $360^\circ$  rotation was complete. In the case of full disk image sequences, that was the end of the pipeline. For the flare cutout image sequences, cutouts were made during each rotation of the full



disk image sequence.

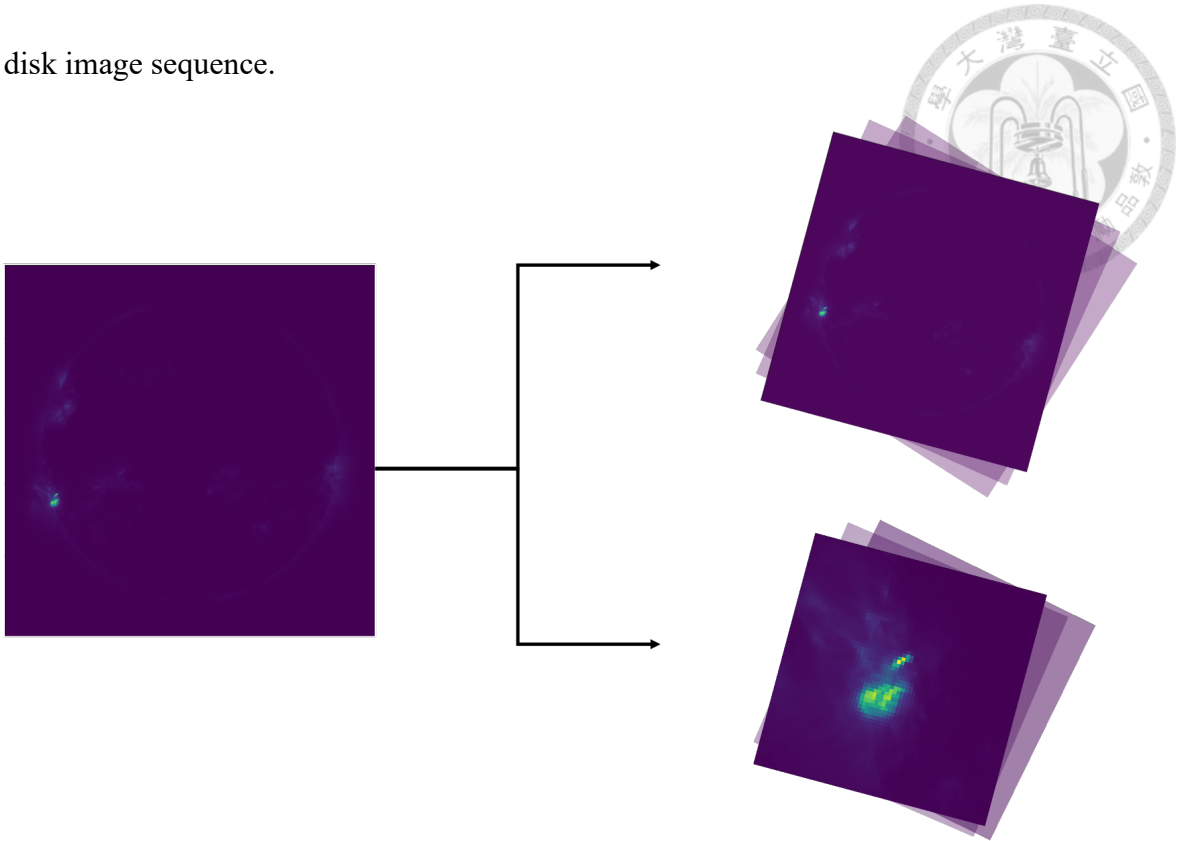


Figure 3.3: Single frame data augmentation visual

Table 3.2: Number of flare event image sequences after data augmentation

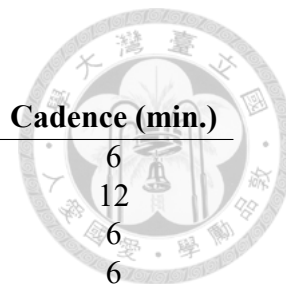
Flare class	Sequences
C	12064
M	17431
X	14256
N	12034
H	18649

### 3.3.4 Datasets

With the ability to create sequences of  $N$  images at any given time  $T$ , and to augment images, we were able to create datasets for training of our models. We created numerous different datasets to test which allows our model to learn the best. Table 3.3 shows the flares included into each dataset. The Hybrid class of flares is a combination of C class flares and Quiet activity. The cadence represents the frequency at which SDO images are taken in minutes.

Table 3.3: Flares included in our datasets

<b>Dataset</b>	<b>Quiet</b>	<b>C Flares</b>	<b>M Flares</b>	<b>X Flares</b>	<b>Hybrid</b>	<b>Cadence (min.)</b>
NCMX6	✓	✓	✓	✓		6
NCMX12	✓	✓	✓	✓		12
NMX6	✓		✓	✓		6
HMX6			✓	✓	✓	6





## Chapter 4 Methods

### 4.1 Goal

The goal of our method is when given a set of full sun *MLDSO* images, automatically detect, classify and determine the flares full duration. Moreover, we would like to extract the flaring region, with the flare at the center of the frames.

### 4.2 Convolutional LSTM

A Convolutional LSTM is an extension of a Fully-Connected LSTM model which uses convolution to capture spatiotemporal relationships of image sequences. In contrast to the original LSTM cells, a ConvLSTM uses convolution on its inputs, allowing it to learn spatial information.

Referencing the original research [21], a ConvLSTM can be formulated as:

$$\begin{aligned}i_t &= \sigma(W_{xi}x_t + W_{hi}h_{t-1} + W_{ci} \circ c_{t-1} + b_i) \\f_t &= \sigma(W_{xf}x_t + W_{hf}h_{t-1} + W_{cf} \circ c_{t-1} + b_f) \\c_t &= f_t \circ c_{t-1} + i_t \circ \tanh(W_{xc}x_t + W_{hc}h_{t-1} + b_c) \\o_t &= \sigma(W_{xo}x_t + W_{ho}h_{t-1} + W_{co} \circ c_t + b_o) \\h_t &= o_t \circ \tanh(c_t)\end{aligned}$$

Where each of the variables can be seen in the ConvLSTM Cell in Figure 4.1.

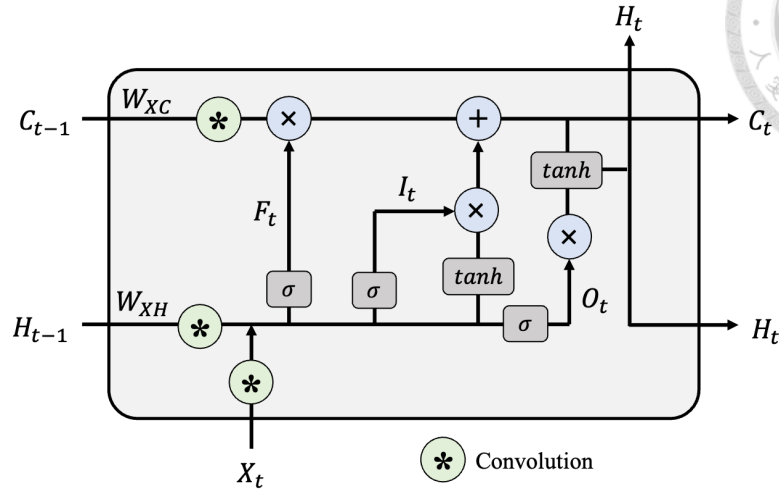


Figure 4.1: A ConvLSTM Cell

### 4.3 Bidirectional Convolutional LSTM

A Bidirectional Convolutional LSTM is essentially the same as the normal ConvLSTM, but the sequences are processed in both forward and backward directions. This allows the model to learn better features, improving performance [7]. Since our research does not focus on prediction of solar flares, we have the ability to process the flare events after they have finished, which is where using Bidirectional ConvLSTMs can be beneficial.

### 4.4 Model Architecture

As seen in figure 4.2, similar to other works that use ConvLSTMs [22, 23], our model stacks multiple Bidirectional ConvLSTM cells. The original authors of the ConvLSTM paper as well as other previous research have shown that by stacking multiple ConvLSTMs in a model increases its complexity, allowing it to learn more elaborate dynamics,

compared to non-stacked ConvLSTM models [11, 21]. The output of the stacked ConvLSTMs is directed into an additional 2D Convolution block, which is then globally pooled and led into a Dense layer, after which a softmax function is used for classification.

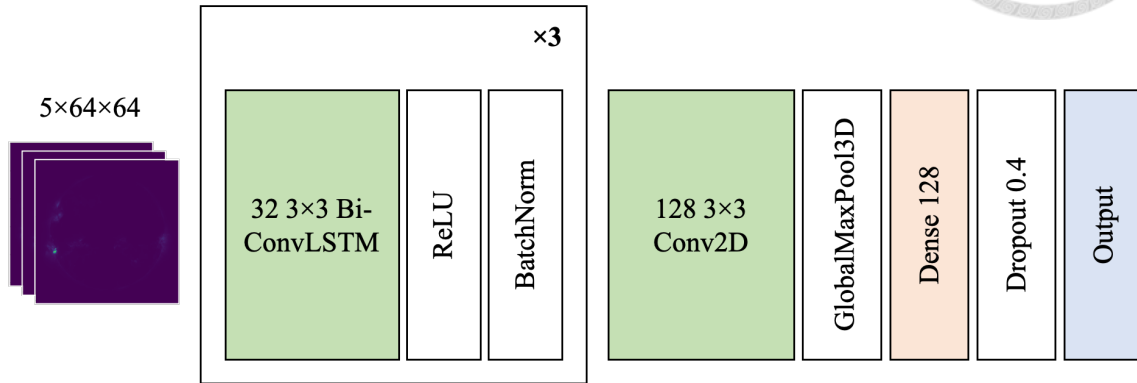


Figure 4.2: Our model architecture

## 4.5 Region Extraction

At the moment a solar flare occurs, it is the most intense magnetic event. We use this fact to detect the region of sun where the flare occurs. When a flare is detected, we use a non-maximal suppression filter on the image of the sun and find the region with the highest intensity. A  $64 \times 64$  pixel bounding box is drawn over that region to encompass the flare.





# Chapter 5 Experiments and Results

## 5.1 Validation Data

Numerous researches dealing with solar flares use a chronological split to test their data [2, 6]. Usually, a specific period of time is chosen as the testing period, such as one year. In this study, we use the year 2013 (excluding August 2013) as a testing year, since all classes (A, B, C, M, X) of solar flares occurred during that year. Hence, we do not use any data from 2013 to train the model, and it is left for testing purposes only.

## 5.2 Evaluation Metrics

Since our model performs both classification and prediction, we break down the evaluation of our model into multiple metrics.

### 5.2.1 Flare Classification

Firstly, we calculate the confusion matrices for flare class classification and use them to calculate the following evaluation metrics:

- Recall

- Precision
- F1 Score



*Note:* The formulas for these evaluation metrics can be found in Appendix B

### 5.2.2 Flare start and end prediction

As mentioned before, there is no dataset which specifically aims to provide information on full flare durations. However, the information about the start and end times of solar flares was retrieved from the HEK. Using our model, we predict the start and end times of the flares, and calculate the difference from the true start and end times retrieved from HEK. The calculation of the flare start and end error can be formulated as follows:

Let our model be denoted as  $M$ , the list of downsampled *MLDSDO* frame differences as  $F$ , the predicted start time of a flare as  $t_{ps}$ , the predicted end time of a flare as  $t_{pe}$ , the true start time of a flare as  $t_{ts}$ , and the true end time of a flare as  $t_{te}$ .

1.  $M$  analyses a sequence of 5 images from  $F$ .
2. If a flare is detected,  $t_{ps}$  is saved.
3. The list of flares is searched for a  $t_{ts}$  closest to  $t_{ps}$ , and the difference between them is saved.
4.  $M$  keeps iterating over  $F$  in a sliding window of width 5 until a flare is no longer predicted,  $t_{pe}$  is saved.
5. The list of flares is searched for a  $t_{te}$  closest to  $t_{pe}$ , and the difference between them is saved.



6. The process continues until  $M$  iterates over the entirety of  $F$ .



## 5.3 Results

The confusion matrices for the trained models can be seen in Figure 5.1. The calculated evaluation metrics can be found in Tables 5.1 through 5.4.

		Predicted		
		H	M	X
Actual	H	0.99	$1 \cdot 10^{-3}$	0
	M	0.43	0.48	0.1
	X	0.25	0	0.75

(a) NMX6 Model

		Predicted		
		H	M	X
Actual	H	0.99	$5.18 \cdot 10^{-3}$	$1.29 \cdot 10^{-3}$
	M	0.53	0.4	$7.5 \cdot 10^{-2}$
	X	0.25	0	0.75

(b) HMX6 Model

		Predicted			
		N	C	M	X
Actual	N	0.78	0.22	$6.45 \cdot 10^{-3}$	$2.58 \cdot 10^{-3}$
	C	0.12	0.88	$5.2 \cdot 10^{-3}$	0
	M	$5 \cdot 10^{-2}$	0.43	0.38	0.15
	X	0	0.25	0	0.75

(c) NCMX6 Model

		Predicted			
		N	C	M	X
Actual	N	0.78	0.21	$3.87 \cdot 10^{-3}$	$3.87 \cdot 10^{-3}$
	C	0.18	0.82	0	0
	M	$5 \cdot 10^{-2}$	0.48	0.33	0.15
	X	0	0.25	0	0.75

(d) NCMX12 Model

Figure 5.1: Confusion Matrices for the tested models of flare start detection. The representations are scaled into a  $[0, 1]$  range. The confusion matrices with raw values can be found in Appendix A.



Table 5.1: Evaluations of the NMX6 model

<b>Flare Class</b>	<b>Precision</b>	<b>Recall</b>	<b>F1 Score</b>	<b>Specificity</b>
H	0.989	0.990	0.989	0.591
M	0.543	0.475	0.507	0.990
X	0.429	0.750	0.545	0.998

Table 5.2: Evaluations of the HMX6 model

<b>Flare Class</b>	<b>Precision</b>	<b>Recall</b>	<b>F1 Score</b>	<b>Specificity</b>
H	0.993	0.964	0.978	0.750
M	0.329	0.625	0.431	0.968
X	0.231	0.750	0.353	0.994

Table 5.3: Evaluations of the NCMX6 model

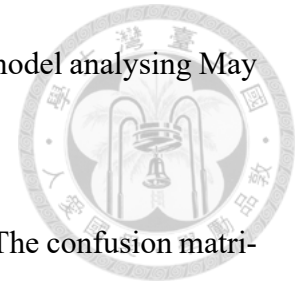
<b>Flare Class</b>	<b>Precision</b>	<b>Recall</b>	<b>F1 Score</b>	<b>Specificity</b>
N	0.867	0.775	0.819	0.887
C	0.784	0.877	0.828	0.774
M	0.625	0.375	0.469	0.994
X	0.273	0.750	0.400	0.995

Table 5.4: Evaluations of the NCMX12 model

<b>Flare Class</b>	<b>Precision</b>	<b>Recall</b>	<b>F1 Score</b>	<b>Specificity</b>
N	0.812	0.781	0.796	0.827
C	0.774	0.820	0.796	0.775
M	0.812	0.325	0.464	0.998
X	0.250	0.750	0.375	0.994

Since the NMX6 model performed the best relative to others, it was used for the flare start and end detection. The average errors for the tested months of 2013 can be seen in

table 5.5. Additionally, a link to a demonstration video showing the model analysing May of 2013 can be found in Appendix A.



Additionally, models for classifying flare cutouts were trained. The confusion matrices for these models can be found in Figure 5.2. The Evaluations can be found in Tables 5.6 and 5.7.

When comparing our models' ability to detect ends of solar flares with Reep *et al.* [18], our models' performance is more volatile. However, there are significant differences with the two approaches. Our model aims to detect the start of the flare as well as the end, and only using image data. Reep *et al.* [18] use physical features and predict the end of the flare only, starting from the peak of the flare.

		Predicted		
		H	M	X
Actual	H	0.92	$7.6 \cdot 10^{-2}$	$1 \cdot 10^{-3}$
	M	0.2	0.78	$2.5 \cdot 10^{-2}$
	X	0.25	0.25	0.5

(a) NMX6 Model

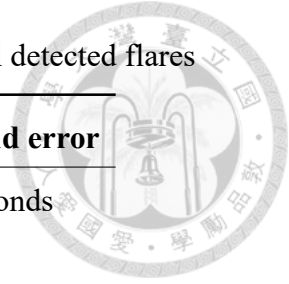
		Predicted		
		H	M	X
Actual	H	0.96	$4.4 \cdot 10^{-2}$	0
	M	0.38	0.53	0.1
	X	0	0.25	0.75

(b) HMX6 Model

Figure 5.2: Confusion Matrices for the tested models of flare start detection cutouts. The representations are scaled into a  $[0, 1]$  range. The confusion matrices with raw values can be found in Appendix A.

Table 5.5: Average errors for flare start and end predictions of all detected flares

<b>Month</b>	<b>Average flare start error</b>	<b>Average flare end error</b>
January	10 minutes	9 minutes 45 seconds
February	4 minutes	10 minutes
March	44 minutes 30 seconds	5 minutes 30 seconds
April	22 minutes	7 minutes 20 seconds
May	17 minutes 32 seconds	12 minutes 36 seconds





## Chapter 6 Conclusion

In this paper, we introduce a novel concept of utilizing only images to perform a full range of tasks involving flare detection, classification, full flare duration, and region extraction. Current research about the solar flares deals mostly with binary prediction of whether or not a flare will occur at a specific active region. Numerous studies use large windows of 24 hours ahead of the flare, as well as some physical features of the flares, whereas we use only a 36 minute window of images from the Machine Learning Dataset Prepared From the NASA Solar Dynamics Observatory Mission. Our model successfully detects flares for their approximate duration. Although this work lays a foundation, the current models classification could be improved. For future work, developing a model which can combine physical features with images may be a viable direction. Moreover, as the current work operates post-flare, a model could be developed to predict the flare, besides classification and full duration prediction.

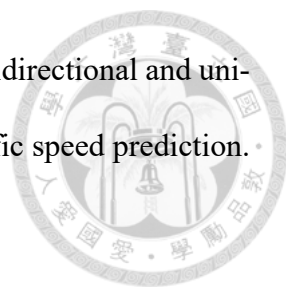


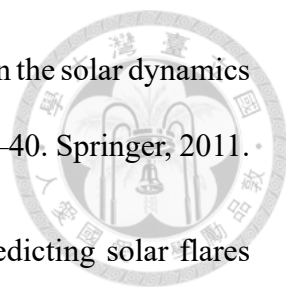


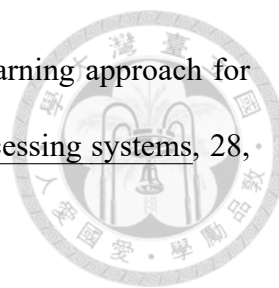


## References

- [1] The Impact of Flares. <https://hesperia.gsfc.nasa.gov/rhessi3/mission/science/the-impact-of-flares/index.html>. Accessed September 4, 2022.
- [2] Ali K Abed, Rami Qahwaji, and Ahmed Abed. The automated prediction of solar flares from sdo images using deep learning. Advances in Space Research, 67(8):2544–2557, 2021.
- [3] AK Aniyani and Kshitij Thorat. Classifying radio galaxies with the convolutional neural network. The Astrophysical Journal Supplement Series, 230(2):20, 2017.
- [4] John A Armstrong and Lyndsay Fletcher. Fast solar image classification using deep learning and its importance for automation in solar physics. Solar Physics, 294(6):1–23, 2019.
- [5] Ji-Hye Baek, Sujin Kim, Seonghwan Choi, Jongyeob Park, Jihun Kim, Wonkeun Jo, and Dongil Kim. Solar event detection using deep-learning-based object detection methods. Solar Physics, 296(11):1–15, 2021.
- [6] Yang Chen, Ward B Manchester, Alfred O Hero, Gabor Toth, Benoit DuFumier, Tian Zhou, Xiantong Wang, Haonan Zhu, Zeyu Sun, and Tamas I Gombosi. Identifying solar flare precursors using time series of sdo/hmi images and sharp parameters. Space Weather, 17(10):1404–1426, 2019.

- 
- [7] Zhiyong Cui, Ruimin Ke, Ziyuan Pu, and Yinhai Wang. Deep bidirectional and unidirectional lstm recurrent neural network for network-wide traffic speed prediction. arXiv preprint arXiv:1801.02143, 2018.
- [8] Richard Galvez, David F Fouhey, Meng Jin, Alexandre Szenicer, Andrés Muñoz-Jaramillo, Mark CM Cheung, Paul J Wright, Monica G Bobra, Yang Liu, James Mason, et al. A machine-learning data set prepared from the nasa solar dynamics observatory mission. The Astrophysical Journal Supplement Series, 242(1):7, 2019.
- [9] N Hurlburt, M Cheung, C Schrijver, L Chang, S Freeland, S Green, C Heck, A Jaffey, A Kobashi, D Schiff, et al. Heliophysics event knowledgebase for the solar dynamics observatory (sdo) and beyond. In The Solar Dynamics Observatory, pages 67–78. Springer, 2010.
- [10] Eric Jonas, Monica Bobra, Vaishaal Shankar, J Todd Hoeksema, and Benjamin Recht. Flare prediction using photospheric and coronal image data. Solar Physics, 293(3):1–22, 2018.
- [11] Seongchan Kim, Seungkyun Hong, Minsu Joh, and Sa-kwang Song. Deeprain: ConvLstm network for precipitation prediction using multichannel radar data. arXiv preprint arXiv:1711.02316, 2017.
- [12] Ahmet Kucuk, Berkay Aydin, and Rafal Angryk. Multi-wavelength solar event detection using faster r-cnn. In 2017 IEEE International Conference on Big Data (Big Data), pages 2552–2558. IEEE, 2017.
- [13] James R Lemen, David J Akin, Paul F Boerner, Catherine Chou, Jerry F Drake, Dexter W Duncan, Christopher G Edwards, Frank M Friedlaender, Gary F Heyman,

- 
- Neal E Hurlburt, et al. The atmospheric imaging assembly (aia) on the solar dynamics observatory (sdo). In The solar dynamics observatory, pages 17–40. Springer, 2011.
- [14] Hao Liu, Chang Liu, Jason TL Wang, and Haimin Wang. Predicting solar flares using a long short-term memory network. The Astrophysical Journal, 877(2):121, 2019.
- [15] Šimon Mackovjak, Martin Harman, Viera Maslej-Krešňáková, and Peter Butka. Scss-net: solar corona structures segmentation by deep learning. Monthly Notices of the Royal Astronomical Society, 508(3):3111–3124, 2021.
- [16] W Dean Pesnell, B J Thompson, and PC Chamberlin. The solar dynamics observatory (sdo). In The solar dynamics observatory, pages 3–15. Springer, 2011.
- [17] Ming Qu, Frank Y Shih, Ju Jing, and Haimin Wang. Automatic solar flare detection using mlp, rbf, and svm. Solar Physics, 217(1):157–172, 2003.
- [18] Jeffrey W Reep and Will T Barnes. Forecasting the remaining duration of an ongoing solar flare. Space Weather, 19(10):e2021SW002754, 2021.
- [19] Shaoqing Ren, Kaiming He, Ross Girshick, and Jian Sun. Faster r-cnn: Towards real-time object detection with region proposal networks. Advances in neural information processing systems, 28, 2015.
- [20] Philip Hanby Scherrer, Jesper Schou, RI Bush, AG Kosovichev, RS Bogart, JT Hoeksema, Y Liu, TL Duvall, J Zhao, CJ Schrijver, et al. The helioseismic and magnetic imager (hmi) investigation for the solar dynamics observatory (sdo). Solar Physics, 275(1):207–227, 2012.
- [21] Xingjian Shi, Zhoung Chen, Hao Wang, Dit-Yan Yeung, Wai-Kin Wong, and



Wang-chun Woo. Convolutional lstm network: A machine learning approach for precipitation nowcasting. Advances in neural information processing systems, 28, 2015.

- [22] Shashwat Singh, Ankul Prajapati, and Kamlesh N Pathak. Predicting future astronomical events using deep learning. arXiv preprint arXiv:2012.15476, 2020.
- [23] Shahroz Tariq, Sangyup Lee, and Simon S Woo. A convolutional lstm based residual network for deepfake video detection. arXiv preprint arXiv:2009.07480, 2020.
- [24] The SunPy Community, Will T. Barnes, Monica G. Bobra, Steven D. Christe, Nabil Freij, Laura A. Hayes, Jack Ireland, Stuart Mumford, David Perez-Suarez, Daniel F. Ryan, Albert Y. Shih, Prateek Chanda, Kolja Glogowski, Russell Hewett, V. Keith Hughitt, Andrew Hill, Kaustubh Hiware, Andrew Inglis, Michael S. F. Kirk, Sudarshan Konge, James Paul Mason, Shane Anthony Maloney, Sophie A. Murray, Asish Panda, Jongyeob Park, Tiago M. D. Pereira, Kevin Reardon, Sabrina Savage, Brigitta M. Sipőcz, David Stansby, Yash Jain, Garrison Taylor, Tannmay Yadav, Rajul, and Trung Kien Dang. The sunpy project: Open source development and status of the version 1.0 core package. The Astrophysical Journal, 890:68–, 2020.



# Appendix A — Additional Data

## A.1 Flare data retrieved from HEK

Table A.1: Flare data retrieved from HEK



<b>Data point</b>	<b>Explanation</b>
event_starttime	Time when event starts
event_endtime	Time when event ends
fl_goescls	GOES Flare class
hpc_coord	
hpc_bbox	
hrc_coord	
hrc_bbox	
hgc_coord	
hgc_bbox	
event_coordsys	Coordinate system type
hgs_coord	
hgs_bbox	
event_peaktime	Peak time of a flare
active	
ar_noaaclass	Active Region NOAA class
ar_noaanum	NOAA designated Active Region Number
boundbox_c1ur	Coord1 of upper-right corner of bounding box
boundbox_c2ur	Coord2 of upper-right corner of bounding box
boundbox_c1ll	Coord1 of lower-left corner of bounding box
boundbox_c2ll	Coord2 of lower-left corner of bounding box
hpc_y	
hpc_x	
hgs_y	
hgs_x	
hpc_radius	
event_c2error	Uncertainty in Coord2 of the mean location of the event.

*Note:* Definitions taken from the official Heliophysics Events Knowledgebase [9] website, [https://www.lmsal.com/hek/VOEvent\\_Spec.html](https://www.lmsal.com/hek/VOEvent_Spec.html)

## A.2 Raw Confusion Matrices





		Predicted		
		H	M	X
Actual	H	1,556	16	0
	M	17	19	4
	X	1	0	3

(a) NMX6 Model

		Predicted		
		H	M	X
Actual	H	1,516	51	5
	M	10	25	5
	X	1	0	3

(b) HMX6 Model

		Predicted			
		N	C	M	X
Actual	N	601	167	5	2
	C	90	673	4	0
	M	2	17	15	6
	X	0	1	0	3

(c) NCMX6 Model

		Predicted			
		N	C	M	X
Actual	N	605	164	3	3
	C	138	629	0	0
	M	2	19	13	6
	X	0	1	0	3

(d) NCMX12 Model



### A.3 A demonstration video

<https://www.youtube.com/watch?v=fH44huGpk-g>







# Appendix B — Formulas

## B.1 Evaluation Metric Formulas

Precision

$$\frac{TP}{TP + FP}$$

Recall

$$\frac{TP}{TP + FN}$$

F1 Score

$$\frac{TP}{TP + \frac{1}{2}(FP + FN)}$$